ON DEPTH-DOSE DISTRIBUTIONS FOR FALLOUT AND SIMULATED FALLOUT FIELDS

R. L. FRENCH
Radiation Research Associates, Inc.,
1506 W. Terrell Ave.,
Fort Worth, Texas 76104,
U.S.A.

and

C. W. GARRETT
Armed Forces Radiobiology Research Institute,
Defense Atomic Support Agency,
Bethesda, Maryland 20034,
U.S.A.

Abstract—Gamma-ray depth-dose patterns in a phantom exposed to fallout were calculated by the Monte Carlo method. The phantom consisted of a tissue equivalent vertical right cylinder 60 cm in height and 30 cm in diameter. The center of the phantom was 111.8 cm above a smooth ground surface uniformly contaminated with ^{235}U fission products. The energy and angular distribution of the gamma rays incident upon the phantom were taken from a previous Monte Carlo study.

The depth-dose patterns were found to be relatively insensitive to fallout age over the period investigated (1 hr to 9 days). The dose rate at the center of the phantom is approximately 65% of the free-field dose rate, while that at the lateral surface is approximately 80%. Except near the extremities, the dose rate along the vertical axis of the phantom varies at approximately the same rate with height above ground as does the free-field dose rate. Approximately one-half of the dose rate at the center of the phantom is from photons which have suffered previous collisions in the phantom.

The depth-dose patterns were also calculated for two arrangements of artificial sources which, although not duplicating the fallout energy spectra, were intended to simulate fallout biological effects. The patterns produced by revolving the phantom on its vertical axis while exposed to a point ^{60}Co source at a horizontal distance of 61 m are similar to those from the fallout, except for internal positions near the bottom of the phantom. A special arrangement of ^{60}Co, ^{137}Cs and ^{144}Ce sources produced substantially the same depth-dose patterns throughout the phantom as did the fallout.

INTRODUCTION

The possible exposure of populations to radioactive fallout has motivated numerous studies of the characteristics of the radiation environment produced by fallout.[1-4] Most of these studies have been concerned with the free-field dose rates and the energy and angular spectra of the gamma-ray flux at a reference height of approximately one meter above a contaminated ground surface. The present study is concerned with calculating the distribution of the gamma-ray dose within a phantom representative of a body exposed to fallout. Because the radiobiologist in investigating the effects of radiation upon biological systems must often perform experiments in simulated radiation fields, the study included depth-dose distributions produced by simulated fallout radiation fields.

A Monte Carlo approach was selected for performing the depth-dose calculations because

it allows a more accurate treatment of the radiation environment and of the geometry of the phantom than do the more rigorous analytic methods for solving the radiation transport problem. However, to provide guidance for the Monte Carlo calculations and to establish the validity of a simpler method, calculations were also performed using exponential attenuation and infinite medium dose buildup factors.

PHANTOM

The phantom consisted of a tissue equivalent vertical right cylinder 60 cm in height and 30 cm in diameter. The center of the phantom was 111.8 cm above the ground surface. For tissue equivalence, the phantom was composed of a homogeneous mixture of the elements indicated in Table 1.

RADIATION ENVIRONMENTS

The fallout radiation environments for which depth-dose distributions in the phantom were calculated were those previously computed by Monte Carlo techniques for a position 0.914 m (3 ft) above fallout with ages of 1.12 hr, 23.8 hr, 4.57 days and 9.82 days uniformly deposited on a smooth ground surface.[3] The fallout was assumed to consist of non-volatile ^{235}U fission products with gamma-ray energy spectra as given by Nelms and Cooper.[5] The simulated fallout radiation environments were those produced by a point isotropic ^{60}Co source (~1.25 MeV) at a horizontal separation distance of 61 m (200 ft), and by a special arrangement of ^{60}Co, ^{137}Cs (~0.67 MeV), and ^{144}Ce (~0.10 MeV) sources known as the AFRRI Compact Simulator.[6]

The geometries of the various radiation sources to which the phantom was exposed are illustrated in Fig. 1. The separation distance of the ^{60}Co point source was selected to give the best approximation of the energy and angular distribution from an infinite plane fallout source.

The AFRRI Compact Simulator, which is a conceptual design, consists of a uniform disc source located on the ground surface, a ring source above the perimeter of the disc source, and a slab of water of equal radius positioned above and concentric with the disc and ring sources. The ring source serves as a virtual source for that portion of an infinite plane source not represented by the disc source while the water serves as a scattering medium for gamma-rays from both the disc and ring source to simulate skyshine from an infinite plane source. The relative concentrations of the ^{60}Co, ^{137}Cs and ^{144}Ce in the disc and ring sources and the thickness of the water slab were selected to give the best approximation of the energy and angular distributions 0.914 m above a 1.12-hr fallout source.

The previous Monte Carlo calculations of the gamma-ray environments produced by the above sources give the total photon flux at the receiver in each of eighteen 10-degree intervals on polar angle, θ, and in each of ten energy groups: 0.04–0.06, 0.06–0.10, 0.10–0.18, 0.18–0.30, 0.30–0.50, 0.50–0.75, 0.75–1.00, 1.00–1.50, 1.50–2.50, and 2.50–3.50 MeV.[3, 6] The fluxes are, for all sources, integrated over azimuthal angle, ϕ. Thus, the environment computed for the ^{60}Co point source is that which would be experienced by revolving the subject about its vertical axis during exposure.

The characteristics of the fallout and simulated fallout radiation environments are illus-

Table 1. Composition of Tissue Equivalent Phantom

Element	% by weight	Partial density (g cm^{-3})	Atomic concentration (atoms cm^{-3})
Carbon	15.6	0.1585	7.944×10^{21}
Hydrogen	9.8	0.0996	5.948×10^{22}
Oxygen	71.0	0.7214	2.714×10^{22}
Nitrogen	3.6	0.0366	1.573×10^{21}
Total	100.0	1.0161	9.614×10^{22}

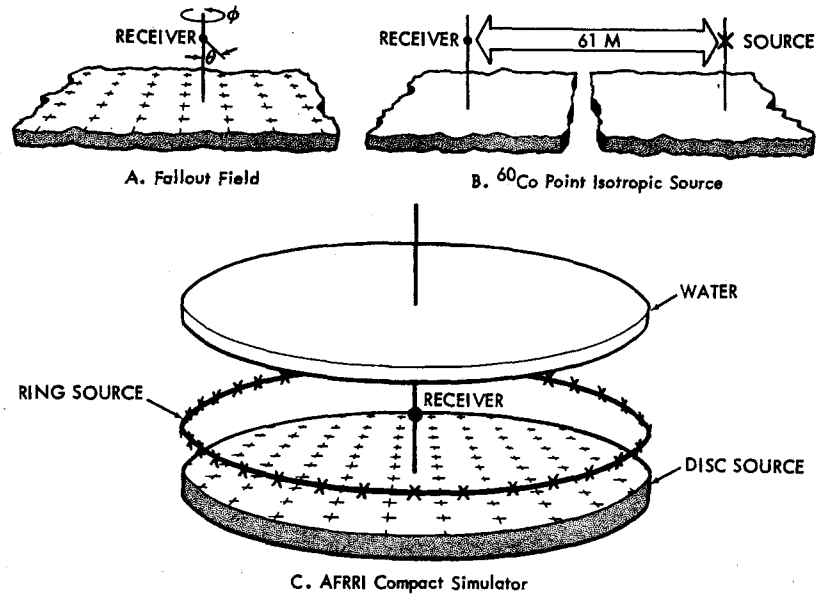

FIG. 1. Source geometries used in free-field radiation environment calculations.

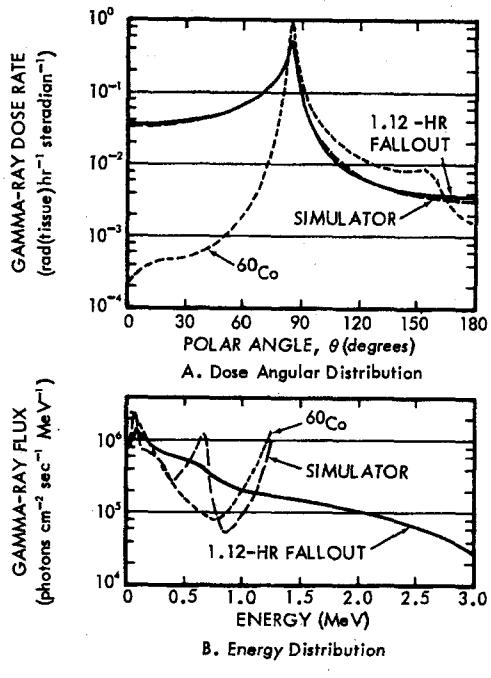

FIG. 2. Gamma-ray energy and angular distributions from 1.12-hr fallout, ^{60}Co point source and AFRRI Compact Simulator (normalized to unit dose rate).

trated in Fig. 2. The angular distributions of the total dose rate, given in the upper part of the figure, have the same gross shape for $\theta > 80$ degrees; but below 80 degrees, the ^{60}Co point source dose angular distribution bears no resemblance to that from fallout. Neither the AFRRI Compact Simulator nor the ^{60}Co point source provides a good simulation of the energy spectra as may be seen in the lower part of the figure.

CALCULATIONAL METHODS

In order to compute the distribution of the gamma-ray dose in the phantom it is necessary to consider the gamma-rays incident over its entire surface and their transport until they are absorbed in, or escape from, the phantom. Actually, photons which escape the phantom may be scattered back into it, but this effect is very small and its neglect is consistent with the neglect of perturbation by the phantom in performing the free-field calculations. In performing the radiation transport calculations, the energy dependent photon flux must be determined at a suitable number of positions in the phantom to allow, after conversion to dose, construction of dose or dose fraction profiles.

The Monte Carlo procedure which was used to perform the transport calculations is a multipurpose code known as COHORT.[7] Its description here will be limited to those features actually used in this study. Basically, the procedure allows photons to be randomly sampled from arbitrary source probability distributions in energy, angle and space. Individual photons are then traced through a random walk generated by sampling from collision probability distributions and angular scattering distributions for the particular materials being penetrated. The collision probability distributions are generated from consideration of the cross sections for Compton scattering, pair production, and absorption. Absorption is not allowed to occur. Instead, the photon weight is reduced upon each interaction by the probability that that particular interaction was an absorption. The angular scattering distributions are generated from the well-known Klein–Nishina formula. Each photon history is terminated upon reaching a specified minimum energy, a specified maximum number of collisions, or escaping from the defined geometry.

An adequate number of photon histories must be traced to assure a representative sampling from the source distributions and a representative distribution of photon interactions. In the process of tracing photon histories, the location of each interaction and the resultant photon energy and direction are recorded on tape. The resultant "collision tape" may then be analyzed to determine the photon track length in arbitrarily specified volume regions. Photon fluxes are obtained by dividing by the volume of the region. Finally, flux-to-dose conversion factors[8] are applied and a summation made over photon energy.

Ideally, the volume regions would be of infinitesimal size to obtain the highest resolution of the spatial dependence of the dose. If valid results are to be obtained, however, each region must be finite and large enough for each to intercept a statistically significant number of photons. Figure 3 shows the volume regions into which the phantom was divided for the COHORT Monte Carlo calculations. The volume regions are concentrated along the horizontal midplane and the vertical axis since it was desired to compute the radial and axial distributions of the dose. The dimensions of the volume elements are smallest near the phantom surface where the largest dose gradients were expected.

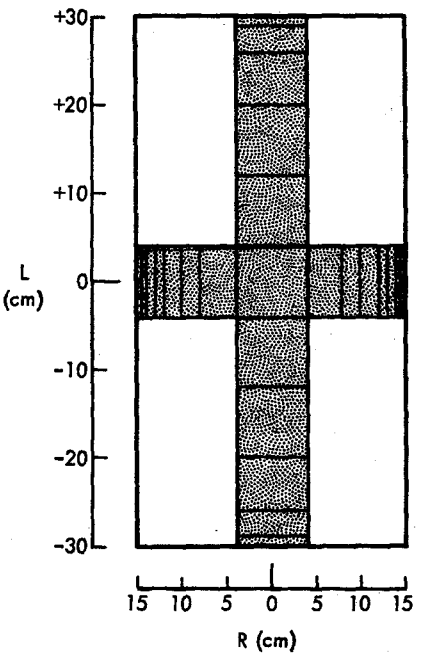

FIG. 3. Division of phantom into volume regions for Monte Carlo calculations.

The source probability distributions on energy and angle were developed directly from the flux tables from the free-field radiation environment calculations. It was assumed that the energy and angular distribution did not vary with height above ground over the length of the phantom. However, the variation of the total incident flux with height was considered too great to be neglected. Special calculations of the total flux above a 1.25-MeV plane isotropic source showed that it varied by 12% over the height of the phantom. In the depth-dose calculations it was assumed that the incident flux from all of the sources except the ^{60}Co point source had a similar height dependence.

In performing the Monte Carlo calculations, each photon was allowed to undergo 15 collisions or be degraded in energy to less than 0.04 MeV before termination. However, it was found that approximately 96% of all photon

histories were terminated by escape from the phantom. Only 3% and 1% were terminated by minimum energy and maximum number of collisions, respectively. An average of only 3.8 collisions were suffered by each photon before its history was terminated.

Exploratory calculations led to the selection of 10,000 photon histories as the minimum problem size to give acceptable statistical accuracy. To further improve the statistical accuracy, four different computer runs using different random number sequences were made for each problem. The final results for most positions in the phantom had standard deviations of less than 5%. No biasing of any type was used in the Monte Carlo calculations.

Prior to the Monte Carlo calculations, exploratory calculations were performed using a simple analytic approach based on exponential attenuation and infinite water medium dose buildup factors[9] for point isotropic sources. For the dose rate at a particular position in the phantom, this type of calculation may be described by the equation

$$D = \sum_{\varphi} \sum_{\theta} \sum_{E} B_E(\mu_E t_{\theta,\varphi}) F_{E,\theta,\varphi} G_E e^{-\mu_E t_{\theta,\varphi}}$$

where
- μ_E is the linear attenuation coefficient of water for photons of energy E,
- $t_{\theta,\varphi}$ is the distance from the dose point to the phantom surface in direction θ and $\varnothing$,
- $B_E(\mu_E t_{\theta,\varphi})$ is the dose buildup factor for penetration of $\mu_E t_{\theta,\varphi}$ mean free paths of water by photons of energy E,
- $F_{E,\theta,\varphi}$ is the free-field flux with energy E from directions θ and $\varnothing$, and
- G_E is the flux-to-dose conversion factor for photons of energy E.

In order to express the depth-dose distribution in terms of dose fractions, both the Monte Carlo and the analytic results were divided by the free-field dose rate 0.914 m above the ground.

RESULTS AND DISCUSSION

Monte Carlo calculations were performed for 1.12-hr fallout, 23.8-hr fallout, the ^{60}Co point source, and the AFRRI Compact Simulator. The results are summarized in Table 2. Analytic calculations were performed for 4.57-day and 9.82-day fallout in addition to the above sources. The results of the various calculations were analyzed to determine:

1. The general characteristics of the depth-dose distributions in the phantom.
2. The sensitivity of the distributions to fallout age.
3. The extent to which the simulated fallout fields reproduce the fallout depth-dose distributions.
4. The validity of the simplified analytic calculations.

The case of principal interest is the 1.12-hr fallout field since this particular age of fallout has been studied extensively.[2, 3, 6] Figure 4 compares the Monte Carlo and analytic calculations for this case. A total of 44,000 photon histories divided into four machine runs were used in the Monte Carlo calculations. The data points shown in the figure are the average of the four runs and the bars indicate the standard deviation as determined from the results of the individual runs. The standard deviations on the radial distribution are seen to be quite small (~2 to 8%). Owing to the use of much smaller volume regions, the standard deviations on the axial distribution are larger near the bottom and the top of the phantom.

The Monte Carlo results indicate a dish-shaped radial distribution with 81% of the free-field dose near (0.5 cm) the lateral surface of the phantom as compared to 66% at the center. For $-20 < L < +20$ cm, the axial distribution is approximately a straight line which closely follows the height-above-ground dependence of the free-field dose rate.

The fine structure near the upper and lower extremities of the phantom can probably be attributed to the combined effect of the boundaries and of the characteristics of the radiation field. The radiation environment to which the phantom is exposed is so strongly peaked near the horizon ($\theta = 90°$) that most of the flux incident upon the bottom and top is at large angles with respect to the normal to these surfaces. Thus, the uncollided component from

Table 2. Depth-dose Distributions in Phantom based on Monte Carlo Calculations (fraction of free-field dose)

Position L or R (cm)	Source			
	1.12-hr fallout	23.8-hr fallout	AFRRI Compact Simulator	^{60}Co point source
		Radial Distribution		
2.83	0.6571	0.6848	0.6418	0.6684
6.67	0.6701	0.6673	0.6600	0.6828
9.06	0.6955	0.6782	0.6806	0.6997
11.04	0.7126	0.7173	0.7190	0.7236
12.51	0.7621	0.7173	0.7676	0.7540
13.51	0.7687	0.7405	0.7597	0.7584
14.26	0.7967	0.7500	0.7724	0.7717
14.75	0.8114	0.7844	0.7812	0.7740
		Axial Distribution		
−29.5	0.9357	0.9023	0.9132	0.5350
−27.5	0.6744	0.6436	0.6937	0.5976
−23.0	0.7210	0.6836	0.6832	0.6333
−16.0	0.6860	0.6443	0.6393	0.6500
− 8.0	0.6926	0.6452	0.6380	0.6809
0	0.6571	0.6848	0.6418	0.6684
8.0	0.6382	0.6500	0.5818	0.6611
16.0	0.6360	0.6042	0.5859	0.6437
23.0	0.5673	0.5754	0.5615	0.6549
27.5	0.5305	0.5253	0.4873	0.5782
29.5	0.5848	0.4809	0.4618	0.6591

the incident flux is highly attenuated in penetrating to positions near the ends of the phantom, giving rise to the relatively strong negative gradient just inside the surface. At the same time, the scattered dose from the much larger number of photons incident upon the sides of the phantom would be expected to decrease near the end surfaces.

The analytic results differ from the Monte Carlo results in two respects:

1. They tend to give slightly higher (~8%) dose fractions in the central regions of the phantom.
2. They do not exhibit the fine structure near the upper and lower extremities.

It was expected that the analytic calculations would generally overpredict the dose fractions owing to the use of infinite medium buildup factors. It is perhaps surprising that the overprediction was no larger since the Monte Carlo calculations indicated that the average photon undergoes only 3.8 collisions before escaping from the phantom. Since the analytic calculations indicated that approximately 50% of the dose near the center of the phantom is from uncollided photons, a component which should contain little error, the 8% difference in the total dose fractions noted above may be attributed to the scattered component alone. This corresponds to an overestimate of approximately 16% in the scattered component of the analytic calculations.

In the analytic results it may be presumed that the absence of fine structure near the upper and lower extremities is a consequence of using infinite medium buildup factors. The excellent agreement between the analytic and Monte Carlo radial distributions near the lateral surfaces is fortuitous; the analytic calculations

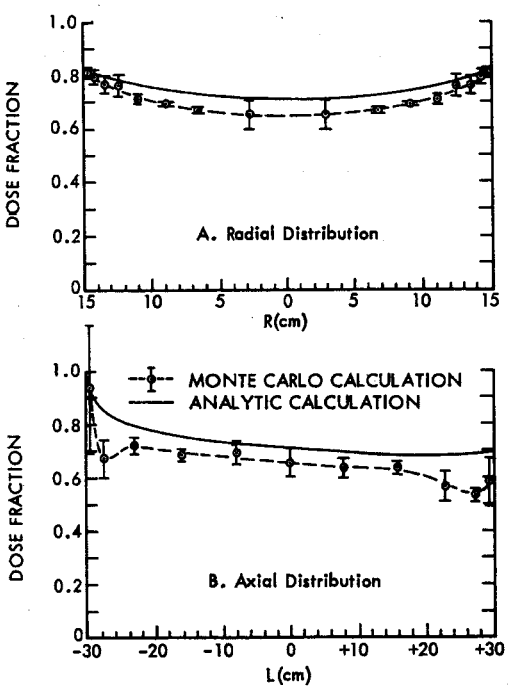

FIG. 4. Depth-dose distribution in phantom exposed to 1.12-hr fallout field.

underpredict the dose fraction in these positions, relative to the central positions, because they do not include reflection of photons from deeper within the phantom.

Figure 5 shows the Monte Carlo calculated depth-dose distributions for the phantom exposed to 23.8-hr fallout. A smoothed curve approximation of the Monte Carlo results for 1.12-hr fallout is included for comparison. The 23.8-hr results, which are based on 40,000 photon histories, tend to be slightly lower near the phantom surfaces and higher near the center than did those for the 1.12-hr fallout. However, it must be concluded that within the statistical accuracy of the results, the two ages of fallout produce essentially identical depth-dose distributions in the phantom. This conclusion is supported by the analytic results (not shown) which differed by not more than approximately 1% at any point in the phantom from those computed for the 1.12-hr fallout.

Originally it was planned to perform Monte Carlo calculations for two additional ages of fallout: 4.57 and 9.82 days. These ages were not considered in the final calculations because their energy spectra do not differ from that of 1.12-hr fallout as much as does that of 23.8-hr fallout, which was found to produce essentially the same depth-dose distributions as 1.12-hr fallout. Moreover, analytic calculations performed for the two additional ages of fallout are within approximately 1% of those for the earlier ages.

The depth-dose distributions produced by a 1.12-hr fallout field simulated by the AFRRI Compact Simulator are compared with those from 1.12-hr fallout in Fig. 6. The radial distribution from the simulator is similar to that for the actual 1.12-hr fallout. The axial distribution is also similar but is slightly lower than that from the fallout. The simulator results shown in Fig. 6 are based on Monte Carlo calculations using 40,000 photon histories. The depth-dose distributions for the AFRRI Compact Simulator computed with the simple analytic method were found to be within 2% of the analytic results for the 1.12-hr fallout.

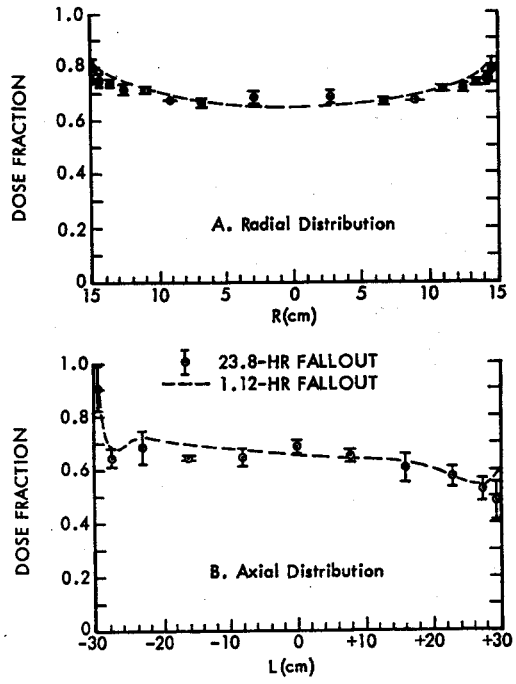

FIG. 5. Comparison of depth-dose distributions for 23.8-hr and 1.12-hr fallout.

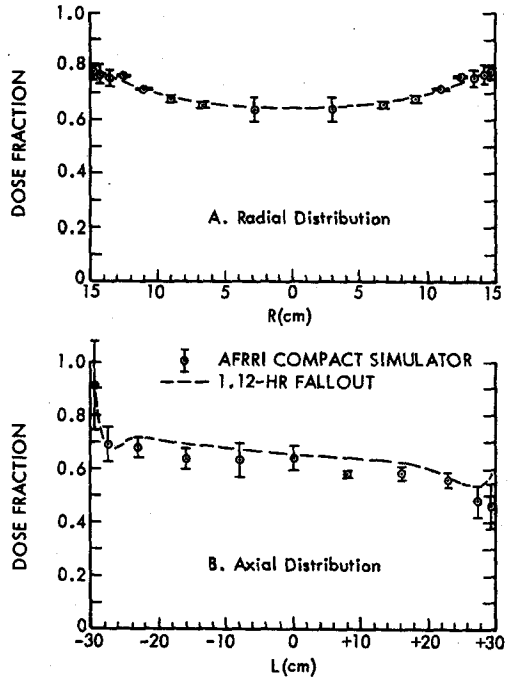

FIG. 6. Comparison of depth-dose distributions for AFRRI Compact Simulator and 1.12-hr fallout.

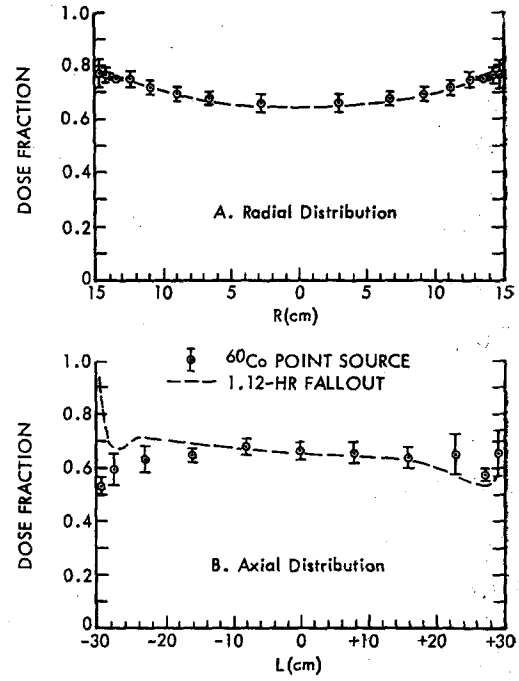

FIG. 7. Comparison of depth-dose distributions for ^{60}Co point source and 1.12-hr fallout.

Figure 7 compares the depth-dose distributions produced by the ^{60}Co point source at a horizontal separation distance of 61 m from the phantom with those produced by 1.12-hr fallout. The radial distribution from the ^{60}Co point source agrees very well in both shape and magnitude with that from the fallout. The axial distribution for the ^{60}Co is also similar to that from the fallout for $-20 < L < +20$ cm. The ^{60}Co dose fraction is lower near the bottom of the phantom because the bottom surface is not exposed to a strong uncollided component as is the case with fallout. However, this difference is probably of trivial significance since the concept of a cylindrical phantom is least valid near the axial extremities. Forty thousand photon histories were used for the ^{60}Co Monte Carlo calculations. Analytic calculations for the ^{60}Co agreed with the Monte Carlo calculations to about the same extent as they did for the other sources.

Although the depth-dose distributions from fallout are simulated reasonably well except near

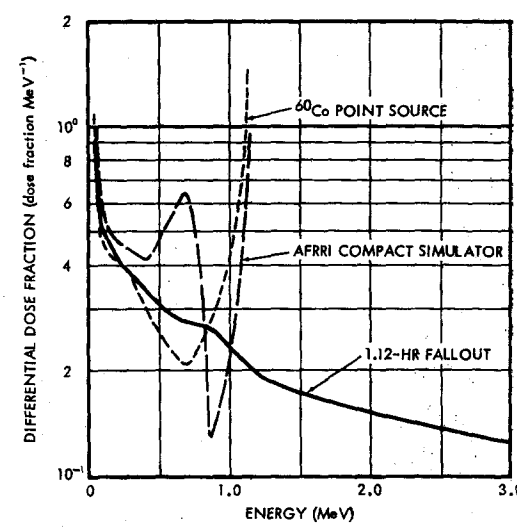

FIG. 8. Differential energy distribution of dose fraction at center of phantom.

the axial extremities by both the AFRRI Compact Simulator and by the ^{60}Co point source at a horizontal separation distance of 61 m, it does not necessarily suffice to simulate the depth-dose distributions alone. The energy distribution of the dose at a given point is also of interest. Figure 8 compares the differential energy spectrum of the dose fraction at the center of the phantom based on the Monte Carlo calculations for the 1.12-hr fallout, the AFRRI Compact Simulator, and the ^{60}Co point source. The two simulated dose spectra are vastly different from that produced by fallout at energies above 1 MeV, and they show only a gross similarity below 1 MeV.

CONCLUSIONS

This investigation has shown that the depth-dose distribution in a phantom exposed to a fallout field is quite insensitive to the age of the fallout. In the horizontal midplane the dose ranges from approximately 65% of the free-field dose at the center of the phantom to approximately 80% at the lateral surfaces. The dose fraction along the vertical axis of the phantom varies at approximately the same rate with height above ground as does the free-field dose rate except near the extremities where boundary effects and the characteristics of the radiation field combine to produce strong dose gradients.

A simple arrangement consisting of a single ^{60}Co point source and a sophisticated arrangement of combined ^{60}Co, ^{137}Cs and ^{144}Ce sources were both found to produce depth-dose distributions over the important regions of the phantom which were very similar to those from the fallout although the energy spectra are quite different. Depth-dose distributions calculated with a simple exponential attenuation and infinite medium buildup factor approach show the same general trends as the more sophisticated Monte Carlo calculations, but are approximately 8% higher in the central portions of the phantom and do not have the same behavior near the boundaries.

ACKNOWLEDGEMENTS

The authors are indebted to L. Olmedo, J. H. Price and K. W. Tompkins, all of Radiation Research Associates, for their assistance with various phases of the calculations. A special acknowledgement is due Col. James T. Brennan, formerly director of the Armed Forces Radiobiology Research Institute, for suggesting the investigation.

REFERENCES

1. R. L. Mather, R. F. Johnson and F. M. Tomnovec. *Health Physics* **8,** 245 (1962).
2. L. V. Spencer. Structure shielding against fallout radiation from nuclear weapons. NBS Monograph 42 (1962).
3. R. L. French. *Health Physics* **11,** 369 (1965).
4. C. M. Huddleston, Q. G. Klingler, Z. G. Burson and R. M. Kinkaid. *Health Physics* **11,** 537 (1965).
5. A. T. Nelms and J. W. Cooper. *Health Physics* **1,** 427 (1959).
6. R. L. French. A comparative study of radioactive source arrangements for simulating fallout gamma radiation fields. RRA-T45 (1964).
7. D. G. Collins and M. B. Wells. COHORT, a Monte Carlo program for calculation of radiation heating and transport. RRA-T62, Vols. I–IV (1966).
8. B. J. Henderson. Conversion of neutron or gamma ray flux to absorbed dose rate. XDC 59-8-179 (1959).
9. H. Goldstein and J. E. Wilkins, Jr. Calculations of the penetration of gamma rays. NYO-3075 (1954).